HHS Public Access

Author manuscript

J Invest Dermatol. Author manuscript; available in PMC 2013 April 01.

Published in final edited form as:

J Invest Dermatol. 2012 October ; 132(10): 2430–2439. doi:10.1038/jid.2012.173.

CELLULAR CHANGES THAT ACCOMPANY SHEDDING OF HUMAN CORNEOCYTES

Tzu-Kai Lin, M.D.[1,2], **Debra Crumrine, B.S.**[1], **Larry D. Ackerman, B.A.**[1], **Juan-Luis Santiago, M.D.**[1,3], **Truus Roelandt, M.D. Ph.D.**[1,4], **Yoshikazu Uchida, Ph.D.**[1], **Melanie Hupe, M.S.**[1], **Gemma Fabriàs, Ph.D.**[5], **Jose Luis Abad, Ph.D.**[5], **Robert H. Rice, Ph.D.**[6], and **Peter M. Elias, M.D.**[1]

[1]Dermatology Service, Department of Veterans Affairs Medical Center, and Department of Dermatology, UCSF, San Francisco, CA, USA

[2]Department of Dermatology, National Cheng Kung University Hospital, and Graduate Institute of Clinical Medicine, College of Medicine, National Cheng Kung University, Tainan, Taiwan

[3]Department of Dermatology, Hospital General de Ciudad Real, Universidad de Castilla-La Mancha, Ciudad Real, Spain

[4]Department of Dermatology, Universitair Ziekenhuis Brussel-Vrije Universiteit Brussel, Brussels, Belgium

[5]Department of Biomedicinal Chemistry, Institut de Química Avançada de Catalunya, CSIC, Barcelona, Spain

[6]Department of Environmental Toxicology, UC Davis, Davis, CA, USA

Abstract

Corneocyte desquamation has been ascribed to either: 1) proteolytic degradation of corneodesmosomes (CD); 2) disorganization of extracellular lamellar bilayers; and/or 3) 'swell-shrinkage-slough' (SSS) from hydration/dehydration. To address the cellular basis for normal exfoliation, we compared changes in *lamellar bilayer architecture* and *CD structure* in DSquame® strips from the 1st vs. 5th stripping ('outer' vs. 'mid'-stratum corneum [SC], respectively) from 9 normal adult forearms. Strippings were either processed for standard EM or for ruthenium (Ru-V)- or osmium-tetroxide (Os-V) vapor fixation, followed by immediate epoxy embedment, an artifact-free protocol that to our knowledge is previously unreported. CDs are largely intact in the mid-SC, but replaced by electron-dense (hydrophilic) clefts (lacunae) that expand laterally, splitting lamellar arrays in the outer SC. Some undegraded DSG1/DSC1 redistribute uniformly into corneocyte envelopes (CEs) in the outer SC (shown by proteomics, Z-

Address correspondence to: Peter M. Elias, MD Dermatology Service (190) VA Medical Center 4150 Clement Street San Francisco, CA 94121 TEL: (415) 750-2091 FAX: (415) 750-2106 eliasp@derm.ucsf.edu.

Conflict of Interest: The authors declare no conflict of interest. The data in this manuscript are original and have not been under consideration for publication elsewhere, nor has this paper's contents been previously published. All authors have read and approved all versions of this manuscript, its contents, and its submission to the JID. Because the document has 1 color figure, we are willing to pay color publication fees.

stack confocal imaging and immunoEM). CEs then thicken, likely facilitating exfoliation by increasing corneocyte rigidity. In vapor-fixed images, hydration only altered the volume of the *extracellular compartment*, expanding lacunae further separating membrane arrays. During dehydration, air replaced water, maintaining the expanded extracellular compartment. Hydration also provoked degradation of membranes by activating contiguous acidic ceramidase activity. Together, these studies identify several parallel mechanisms that orchestrate exfoliation from the surface of normal human skin.

Keywords

ceramidase; corneodesmosomes; cornified envelope; desmocollin 1; desmoglein 1; desquamation; electron microscopy; lamellar bilayers; ruthenium tetroxide; stratum corneum

INTRODUCTION

In normal human skin, the lower layers of the stratum corneum (stratum compactum) are highly cohesive, a characteristic important for permeability barrier function, antimicrobial defense, and stratum corneum integrity (= resistance to shear forces) (Elias, *et al*., 2005, Cork, *et al*., 2006, Elias, 2007). Stratum corneum (SC) cohesion can be attributed in part to an epidermis-unique, junctional structure, the corneodesmosome (CD), which replaces desmosomes in the SC. As corneocytes migrate apically, CDs are degraded by extracellular kallikreins (serine proteases) as well as cysteine and aspartate proteases (Brattsand, *et al*., 2005, Ovaere, *et al*., 2009, Zeeuwen, *et al*., 2009, Rawlings, 2010) in a pH-dependent fashion (Hachem, *et al*., 2003, Hachem, *et al*., 2005, Gunathilake, *et al*., 2009), yielding the less-compact stratum disjunctum. The putative biochemical correlates of this sequence include the initial proteolysis of an SC-unique protein, corneodesmosin (Lundstrom, *et al*., 1994, Jonca, *et al*., 2011), followed by the sequential proteolysis of other CD constituent proteins, including two e-cadherins, desmoglein 1 (DSG1) and desmocollin 1 (DSC1) (Lundstrom, *et al*., 1990, Caubet, *et al*., 2004). Yet, morphological, biochemical and immunofluorescence studies suggest that CDs, with the possible exception of a subgroup of peripheral CDs (Chapman, *et al*., 1990, Haftek, 2006, Ishida-Yamamoto, *et al*., 2011), are largely degraded before corneocytes arrive in the outer SC (Rawlings, *et al*., 1994). Which further, distal alterations in CD or other cohesion factors (see below) accomplish normal exfoliation is one of the key questions addressed in this study.

While alterations in CD clearly represent a key, but relatively-early desquamatory mechanism, disorganization or degradation of lamellar bilayers could also facilitate desquamation. Although lamellar bilayers reportedly persist unaltered within the outer SC (Madison, *et al*., 1987), inherited disorders of lipid metabolism that are associated with aberrant desquamation (ichthyosis) exhibit altered bilayer composition and structure (Williams, *et al*., 1987, Elias, *et al*., 2008, Elias, *et al*., 2010). Changes in lipid composition across the SC, particularly in cholesterol sulfate content, have been proposed to regulate desquamation (Epstein, *et al*., 1981, Long, *et al*., 1985, Rehfeld, *et al*., 1988). Moreover, mild organic solvent and/or detergent treatment of SC generates individual corneocytes (Chapman, *et al*., 1991, Shukuwa, *et al*., 1997). Because two ceramidase isoforms, acidic

(aCDase) and alkaline CDase are expressed in SC (Wertz, *et al*., 1990, Houben, *et al*., 2006), either or both could account for the substantial amounts of sphingosine and ω-hydroxy fatty acids that are present in SC (Uchida, *et al*., 2008). Whether an attack by ceramidases on lamellar bilayers could degrade lamellar membranes, further facilitating exfoliation, is a second question addressed in this study.

Finally, it has been proposed (but not yet shown) that abrupt changes in surface area:volume ratios that follow hydration (e.g., with bathing) could induce volume shifts in SC subcellular compartments, sufficient to provoke exfoliation by physical forces ('swell-shrink-slough,' SSS) (Williams, 1992, Williams, *et al*., 1993, Elias, *et al*., 2010). Whether hydration induces changes in SC subcellular compartments that could contribute to shedding is a third issue addressed in this study.

Yet, it has been difficult, if not impossible, to address the mechanisms that lead to normal corneocyte detachment, because the SC is unusually susceptible to artifacts that are provoked during fixation and embedding for light and electron microscopy. One such distortion is lipid extraction during tissue processing, which yields the 'normal basket-weave' appearance of SC on light microscopy, images that relegated the SC to functional irrelevance for decades. In frozen sections, the SC instead was subsequently revealed to be exquisitely organized into vertical, interlocking columns of polyhedral cells (Christophers, *et al*., 1964, Menton, *et al*., 1971, Mackenzie, 1975), with SC membrane domains enriched in hydrophobic lipids (Elias, *et al*., 1975, Elias, *et al*., 1977, Grayson, *et al*., 1982, Elias, *et al*., 1983), that are organized into extracellular lamellar bilayers that extend throughout the SC interstices (Hou, *et al*., 1991). Ruthenium tetroxide (RuO_4) immersion post-fixation (Ru-I), developed to examine these domains in epoxy-embedded tissue sections (Madison, *et al*., 1987, Hou, *et al*., 1991), revealed not only extracellular domains replete with lamellar bilayers (Madison, *et al*., 1987), but also that Ru-I post-fixation preserves lamellar bilayer dimensions with fidelity (Hou, *et al*., 1991). Yet, Ru-I and osmium tetroxide immersion post-fixation (Os-I) are routinely preceded by aldehyde pre-fixation, which also produces draconian, hydration-induced alterations in the volume relationships of the cellular (CC) and extracellular (ECC) compartments. Cognizant of these drawbacks, we developed an OsO_4 and RuO4 vapor-phase fixation protocol (Os-V and Ru-V, respectively), followed by immediate epoxy embedding that obviates the need for both prefixation, and immersion in solvents, nullifying the dehydration and extraction artifacts that accompany standard tissue processing. Our results show that exfoliation from the skin surface is orchestrated by multiple, often subtle processes that operate in parallel within the outer SC.

RESULTS

Comparison of SC Structure in Immersion vs. Vapor Fixation Protocols

We initially assessed the efficacy and potential utility of vapor fixation by comparing the ultrastructure of biopsies and/or strippings from nine normal human subjects (suppl. Table 1) that were processed in parallel by standard immersion methods and the vapor fixation protocols. Ru-I revealed multilayered lamellar bilayers that were also well-preserved and readily visualized in Ru-V-fixed samples (Figs. 1B vs. A, arrows). While there were frequent extraction artifacts (empty = electron-lucent spaces) in Ru-I samples, such

extraction artifacts were not observed in Ru-V fixed samples (Figs. 1B vs. A, asterisks), suggesting that Ru-V fixation does not disturb SC volume relationships. Yet, due to its strong oxidant characteristics, neither Ru-I nor Ru-V reliably preserved cornified envelopes (CE) or corneodesmosomes (CD) (Fig. 1). Thus, Ru-V fixation can be employed to visualize the extracellular lamellar bilayers, and both Ru-V and Os-V preserve volume relationships in the SC (Suppl. Table 2).

Immersion fixation with OsO_4 (Os-I), particularly if preceded by pyridine treatment, provides pristine images of CEs, CDs, and the corneocyte lipid envelope (CLE) (Fig. 1c) (Elias, *et al*., 1979, Behne, *et al*., 2000, Elias, *et al*., 2010), but lamellar bilayers cannot be visualized. As with Ru-I, electron-lucent loci, that likely represent extraction artifacts, occur throughout the extracellular matrix in Os-I (universally shown in prior published studies), but not in Os-V treated samples (Fig. 2c). While Os-V post-fixation, like Os-I preserves the CLE, lamellar bilayers again could not be visualized (Fig. 1d). Both CDs and CEs appeared less electron-dense than in parallel Os-I post-fixed tissues (Fig. 1d vs. 1c). Yet, like Ru-V, Os-V fixation appears to preserve ECC dimensions (Fig. 2c, open arrows). Thus, deployment of either Ru-V or Os-V could be utilized for delineation of volume relationships in SC (Suppl. Table 2).

Volume of Extracellular Compartment in Normal and Hydrated SC

The unique susceptibility of SC to dehydration and extraction artifacts during immersion fixation, post-fixation and embedding has impeded prior attempts to assess changes in the volume of the CC and ECC. Hence, we next deployed Os-V and Ru-V fixation to visualize and quantitate changes in the ECC during transition from the mid- to the outer SC in multiple (≥40), randomly-selected micrographs from ≥10 micrographs the nine (9) normal subjects. Under normal (basal) conditions, the volume contribution of the ECC was ≈12% in the mid-SC, increasing to ≈17% in the outer SC, an increase that did not achieve statistical significance (Suppl. Table 3; $p<0.1$).

'Swell, shrink, and slough' (SSS) of corneocytes with hydration followed by drying, could provoke shedding of individual cells, because abrupt shifts in water content could stress cell-to-cell contacts (Williams, 1992, Williams, *et al*., 1993, Elias, *et al*., 2010). Therefore, we next examined the SSS hypothesis by quantitative analysis of Os-V samples (simultaneously visualized with Ru-V), before, immediately after, and 45 min and 2 hrs after hydration. Hydration expanded the ECC in both the mid-SC (from 11.8±0.9% pre-immersion to 20.2±1.4% immediately post-immersion [Suppl. Fig. 1a and Suppl. Table 3; $p<0.001$]), and in the outer SC (from 17.4±1.3% prior to immersion to 20.0±1.6% immediately after immersion [Suppl. Fig. 1a]). Yet, ECC volume remained unchanged at 45 min and 2 hrs post-hydration, because air appeared to replace water as the latter evaporated from the ECC (Fig. 5, asterisks). Changes in the volume of individual corneocytes were assessed quantitatively as corneocyte area/corneocyte length (see Methods). Notably, the volume contribution of the CC did not change before or after hydration in either the mid- or outer SC (Suppl. Fig. 1b). Together, these results show first, that SSS expands the ECC compartment in both the mid- and outer SC, maintaining hydration-induced separation of

adjacent corneocytes; and second, that the CC does not change with hydration of either the mid- or outer SC.

Distal Consequences of Corneodesmosome Degradation

To assess the structural and biochemical alterations that accompany normal shedding, we next assessed changes in CD and CE structure in the mid- and outer SC, in samples exposed to Os-I post-fixation, which optimally preserves both CEs and CDs (Table 1). As noted above, while CDs still appeared largely intact in the mid-SC, all CDs lost their characteristic plug-like structure in the outer SC. Despite the widely-accepted view that a sub-group of CS persist up to skin surface (Haftek, 2006, Naoe, *et al*., 2010, Ishida-Yamamoto, *et al*., 2011), we found no remaining intact CDs in the outer SC of any of our seven human subjects. Instead, CDs appeared to be replaced by lacunar (lenticular) dilatations filled with amorphous, electron-dense material (Figs. 1&2). Because the spacing between these dilatations corresponds to intervals between adjacent CDs, these dilatations likely represent sites of prior CD degradation (Menon, *et al*., 1997, Haftek, 2006). These lacunae then expand in the outer SC, splitting lamellar bilayers into single or double lamellar arrays (see below).

Despite the apparent loss of CD structures during progression from the mid- to outer SC, confocal immunofluorescence images show that both desmoglein 1 (DSG1) and desmocollin 1 (DSC1) continue to exhibit both a granular ‘dot-like’ distribution, and uniform CE labeling in the outer SC (Figs. 3A&B). While it has been proposed that these proteins concentrate in residual (intact) CD in the cell periphery (Haftek, 2006, Naoe, *et al*., 2010, Ishida-Yamamoto, *et al*., 2011), the uniform redistribution of much of these proteins to CEs was confirmed in Z-stack images of both DSG1 and DSC1 labeled samples (Fig. 3a), and by immunoelectron microscopy (IEM) (Figs. 3C+D [negative controls showed no immunolabeling]). Moreover, DSG1 immunogold labeling revealed diffuse labeling of CEs; i.e., there was no increase at the cell periphery that would indicate concentration of this protein in ‘peripheral’ CDs (Fig. 3c, insert). Thus, a decrease in corneocyte vertical dimensions in the outer SC, as well as retention of some undegraded DSG1/DSC1 in CD-derived lacunae, likely account for the previously-described ‘peripheral localization’ of these proteins.

Proteomic analysis of samples also suggests that DSG1 and DSC1 are largely redistributed from CDs to CEs. While the unique peptide isoform (DPI) of desmoplakin declined in the outer vs. the mid-SC (Fig. 3e), the DSG1 and DSC1 (isoform 1A) content of CEs increased significantly in the outer SC (Fig. 3c&d), while the content of other CE proteins (e.g., loricrin, keratins 1/10, small poline-rich proteins, transglutaminase 5 and DSC3) did not change in samples from midto outer SC. These results, coupled with the immunofluorescent and immunoelectron microscopy studies, suggest that some DSG1/DSC1 remains in CD-derived lacunae, but some is released intact from CD, and then incorporated into CEs.

If DSG1 and DSC1 are (re)incorporated into CEs, one would expect that CE dimensions would expand accordingly. Hence, we next measured changes in CE dimensions in perpendicular sections during the transition from the mid- to the outer SC. Consistent with the redistribution of a pool of DSG1 and DSC1 to CEs, and the ongoing cross-linking of CE

precursors that continues across the entire SC (Michel, *et al*., 1988, Kalinin, *et al*., 2002, Eckert, *et al*., 2005a, Eckert, *et al*., 2005b), CE thickness increased significantly (by ≈15%) as corneocytes transitioned from the mid- to outer SC (Fig 4A&B). Together, these results suggest that contrary to current dogma, that all CDs are degraded prior to arrival in the outer SC, but that some DSG1/DSC1 remains in lacunar domains, while some is incorporated into CEs.

SSS Provokes Further Changes in Lamellar Bilayer Structure

To assess changes in lamellar bilayer organization and substructure during transition from the mid- to the outer SC, we utilized Ru-V fixation. Under basal (non-hydrated) conditions, lamellar bilayers remain largely intact in the mid-SC (Fig. 5c; cf, Fig. 1b). As CD-derived lacunae expand laterally during transition to the outer SC (*vide supra*), these non-lamellar domains split lamellar multilayers into single or double lamellar arrays (Fig. 5b).

We next assessed whether SSS provokes further alterations in lamellar bilayer sub-structure. Whereas lamellar bilayers in the mid-SC appeared largely unaltered prior to immersion, small punctate discontinuities appeared in lamellar bilayers immediately after immersion, and these alterations persisted 45 min and 2 hr post-immersion (Fig. 5d = 2 hrs post-hydration). Thus, hydration not only disorganizes (splits) lamellar bilayer arrays, but it also appears to provoke degradation of individual lamellae.

Hydration is required to activate various types of hydrolytic enzyme activity, including two ceramidase isoforms present in SC (Wertz, *et al*., 1990, Houben, *et al*., 2006). Ceramidases are the only hydrolases that are known to partially degrade ceramides into sphingoid bases and fatty acids (Uchida, *et al*., 2008). To evaluate whether activation of either ceramidase isoform could account for the hydration-induced lamellar bilayer degradation, we developed a zymographic assay (that to our knowledge is previously unreported) that allows visualization and localization of ceramidase activity under either acidic (pH 4.5) or neutral-to-alkaline (pH 7.8) conditions (Figs. 5E-G). Both acidic and alkaline activities peak in the stratum granulosum, and persist into the SC. Yet, while alkaline activity declines in the outer SC (Fig. 5f), acidic activity not only persists throughout the SC, but also concentrates at the periphery of corneocytes (Fig. 5e). Sections pre-treated with the pan-ceramidase inhibitor, N-oleoylethanolamine (NOE), greatly reduced both enzyme activities (Fig. 5g), verifying enzyme activity in SC membrane domains can be attributed to acidic ceramidase. Together, these results show that hydration accelerates lamellar bilayer disorganization and provokes bilayer degradation by acidic ceramidase in the outer SC.

DISCUSSION

We deploy here an artifact-free vapor fixation protocol (that to our knowledge is previously unreported) to address the basis for shedding from the surface of normal human SC. Standard methods of fixation and embedding produce dehydration and extraction artifacts that shrink and detach corneocytes, even though Ru-I post-fixation preserves lamellar bilayer arrays (Hou, *et al*., 1991, Swartzendruber, *et al*., 1995). Though we show here that vapor fixation preserves extracellular dimensions and SC structures, without inducing artifactual cell separation, Ru-V like Ru-I, is highly reactive, oxidizing protein-enriched

structures, such as CDs and CEs, while in contrast, Os-I (but not Os-V) post-fixation appears to preserve these structures (Suppl. Table 2). We deployed these vapor-phase protocols, that to our knowledge are previously unreported, in conjunction with ultrastructural, immunofluorescent, proteomic and zymographic methods, to evaluate the basis for normal exfoliation, comparing tape strippings from the outermost and mid-SC. Since the 1st stripping removed a variable number of cell layers, we concentrated on changes in the 1st vs. 5th stripping.

Although corneocytes become less cohesive as they progress through the SC [e.g., (King, *et al*., 1979)], how individual corneocytes desquamate from the cell surface is less clear. Serine proteases, particularly kallikreins 5 and 7, are known effectors of desquamation (Egelrud, 2000, Brattsand, *et al*., 2005, Rawlings, 2010). Accordingly, desquamation accelerates at the higher-than-normal pH of inflammatory dermatoses, threatening the cohesion of SC (Hachem, *et al*., 2003, Hachem, *et al*., 2005, Cork, *et al*., 2006, Hachem, *et al*., 2006a, Haftek, 2006, Voegeli, *et al*., 2009). Conversely, desquamation is delayed in parallel with retained CDs and restricted enzyme activity, in x-linked ichthyosis (Elias, *et al*., 2004), where the pH of SC is lower than normal (Ohman, *et al*., 1998). Our observations confirm that CD degradation is an important and likely required antecedent for desquamation, but apparently certain still-later events provoke distal shedding, because all CD are degraded before corneocytes reach the outer SC. Importantly, we did not find a persistent pool of 'peripheral CD' in the outer SC, as described by others (Chapman, *et al*., 1990, Naoe, *et al*., 2010, Ishida-Yamamoto, *et al*., 2011). What has been called CDs instead comprise lacunar domains that appear to occupy sites formerly occupied by CDs (Menon, *et al*., 1997, Haftek, 2006). These lacunae then expand laterally, splitting lamellar bilayers, a process that we show here accelerates following hydration.

Such expansion of lacunar domains, separating lamellar bilayers, likely also facilitates distal shedding (Fig. 6). Thus, the ECC of the SC expands with hydration, and contracts as it loses water. While the absolute volume of the CC does not change with hydration, its relative volume declines as the ECC correspondingly expands. Moreover, as water evaporates following SSS, it appears to be replaced by air, maintaining the expanded volume of the ECC in the outer SC. The expansile characteristics of SC extracellular domains have been noted previously (Nemanic, *et al*., 1980, Rawlings, 2010). Together, this sequence likely sustains gaps between adjacent corneocytes, thereby facilitating intercellular detachment (Fig. 6).

The observation that the volume of the CC does not change with hydration refutes a commonly-held view that it is the *cellular* (rather than the extracellular) compartment that changes with hydration/dehydration [rev. in (Rawlings, *et al*., 1994)]. The inability of corneocytes in the midand outer SC to retain water could be due to the presence of ceramidase activities in the SC (Wertz, *et al*., 1990, Houben, *et al*., 2006), which attack the ω-hydroxy-ceramide monolayer that forms the CLE (Downing, 1992, Uchida, *et al*., 2008). While corneocytes in the lower SC display a replete CLE that likely retains hygroscopic substances, ceramidase-mediated hydrolysis of the CLE should render corneocytes unable to retain hygroscopic molecules; allowing water to move in and out of corneocytes. Thus, the ECC becomes the expansile compartment in the midto outer SC. While these results validate

the SSS hypothesis, the underlying processes do not operate by 'stretch and strain' due to corneocyte swelling and shrinkage, but rather by physical separation of adjacent corneocytes, coupled with disorganization and degradation (see below) of lamellar bilayers.

CD degradation likely contributes to shedding by another, previously-undescribed mechanism. Our immunofluorescent, IEM and proteomic results suggest that much of the proteolytic attack on CD may be directed at proteins, other than DSG1 and DSC1, such as corneodesmosin and desmoplakin, and that their degradation likely accounts for CD degradation. In contrast to *in vitro* studies (Caubet, *et al*., 2004), little or no DSG1 and DSC1 appear to be degraded *in vivo*. Instead, the proteomic, immunofluorescent, immunoEM and ultrastructural data suggest that proteolysis of CDs releases abundant, full-length protein that then is both retained in lacunar domains and partially redistributed uniformly within CEs of the outer SC.[1] Comparable immunofluorescent images have been interpreted by others to indicate that DSG1/DSC1 are retained within a pool of residual, peripheral CD that persist in the outer SC (Naoe, *et al*., 2010, Ishida-Yamamoto, *et al*., 2011). Yet, we did not observe any residual CD in the outer SC in either immersion or vapor-fixed samples. Moreover, our Z-stack images show that the apparent peripheral localization of CD constituent proteins likely represents an optical illusion due to the progressive flattening of corneocytes. Furthermore, the subsequent (re)incorporation of DSG1, DSC1, and likely other CE precursor peptides into the CE also accounts, at least in part, for the uniform increase in thickness of CEs in the outer SC, consistent with the known persistence of CE cross-linking activity in the SC (Michel, *et al*., 1988, Koch, *et al*., 2000, Kalinin, *et al*., 2002, Segre, 2003, Schmuth, *et al*., 2004, Candi, *et al*., 2005, Eckert, *et al*., 2005b, Eckert, *et al*., 2005a). Pertinently, both DSG1 and DSC1 possess potential TG1 binding sites (Haftek, *et al*., 1991, Robinson, *et al*., 1997). CE thickening would not only increase mechanical resistance, but likely also increase envelope rigidity, thereby facilitating individual cell separation ('flaking') immediately prior to shedding of individual corneocytes (Fig. 6).

We also observed changes in extracellular lamellar bilayer organization and substructure that likely contribute to exfoliation. Electron spin resonance (Yagi, *et al*., 2007), Fourier transform infrared (FTIR) (Berthaud, *et al*., 2011), and scanning EM (Lopez, *et al*., 2000) show that lamellar bilayer organization changes in the outer SC, attributed (incorrectly) to the imbibement of sebaceous lipids. We observed here instead splitting of multi-layered stacks of lamellar bilayers into single or double membrane arrays, which likely account for these previously-observed changes. Disorganization (splitting) occurs even under basal (non-hydrated) conditions, but it is further accentuated by SSS. Yet, hydration provoked further alterations in lamellar bilayer structure; i.e., punctate discontinuities in individual membranes consistent with membrane degradation, which could further facilitate shedding (Fig. 6). Indubitably, enzymatic activity increases with hydration, because hydrolases require an aqueous environment for optimal activity. We show here that acidic ceramidase co-localizes to sites where lamellar bilayers show focal degradation. Notably, activities of

[1]It is worth noting that detachment of full-length proteins from the CE is not unprecedented, since filaggrin also is released intact from the CE, prior to its proteolytic degradation (Scott, IR, *et al*., 1986).

another key family of hydrolases: i.e., serine proteases, declines in the outer SC (Hachem, *et al*., 2006b, Gunathilake, *et al*., 2009, Hachem, *et al*., 2010).

MATERIALS AND METHODS

Immersion (Standard) and Vapor Post-Fixation

For vapor fixation, portions of D-Squames were suspended immediately after stripping above either 0.5% aqueous RuO_4 (Polysciences #18253) or 4% aqueous OsO_4 (EMS #19190) in Eppendorf tubes under an exhaust hood at room temperature with no light exposure, care being taken to avoid any contact with the fluid phase. While Ru-V post-fixation was terminated after 2 hrs, Os-V exposure was maintained for 16 hrs. D-Squame pieces then were removed from the tubes, dried under the exhaust hood for 15 min to remove residual RuO_4/OsO_4 vapor, and then cut into still smaller pieces (≤0.5mm diameter), followed by immersion in a freshly-prepared epoxy mixture for one hr. Individual pieces then were stacked together and oriented horizontally in rubber molds. Parallel portions of each stripping were processed by standard immersion methods, including pre-fixation in glutaraldehyde, post-fixation in OsO4 or RuO4, followed by solvent dehydration and epoxy embedding (Hou, *et al*., 1991). All EM samples were polymerized at 80°C overnight, prior to ultrathin sectioning and viewing in a Zeiss 10A electron microscope, operated at 60 KV.

Quantitative Morphology

Measurements of *cornified envelope (CE) dimensions* were performed perpendicular (cross) sections in 10 separate, randomly-obtained images from each stripping from four different male Asian subjects (Table 1), utilizing Gatan Bioscan with DigitalMicrograph™ software. The *volume contribution* of the *cellular (CC)* vs. *extracellular (ECC) compartments* was determined in Ru-V samples by a stereological (morphometric) point-count procedure, which allows quantitative reconstruction of three-dimensional structure from measurements of two-dimensional images (Weibel ER, Elias H 1967). The volume contribution of the ECC (V_{ECC}) vs. the CC (V_{CC}) was determined by randomly superimposing an array of points over images, and quantitating the number (N) of 'hits' that overlie each compartment (> ten randomly-selected micrographs from each tape stripped sample, from each subject [Table 1]). Points that fell in areas of ambiguous or potentially-artifactual (empty) spaces were excluded, except in post-hydration samples where empty spaces appeared at extracellular sites previously occupied by saline. The volume contribution of the ECC was calculated as a percentage of total SC, derived as $N_{ECC} / (N_{ECC} + N_{CC}) \times 100$. A second quantitative procedure was also employed to evaluate the impact of *hydration/dehydration* on *compartment volumes* in strippings from the same four subjects. Changes in the volume of ECC and CC prior to and after immersion were normalized to the cumulative length of cellular borders, determined planimetrically by Map Wheel (Scalex Corp., Carlsbad, CA). Please see Supplemental Material for more Materials and Methods.

Supplementary Material

Refer to Web version on PubMed Central for supplementary material.

Acknowledgements

We gratefully acknowledge the superb editorial assistance of Ms. Joan Wakefield, including her preparation of the graphics. This work was supported by NIAMS/NIH grants AR019098 and P42 ES04699, by the Medical Research Service, Department of Veterans Affairs, San Francisco, and the Foundation for Ichthyoses and Related Skin Types. These contents are solely the responsibility of the authors and do not necessarily represent the official views of the NIAMS or NIH.

Abbreviations

CC	corneocyte compartment
CD	corneodesmosome
CDase	ceramidase isoform
CE	cornified envelope
CLE	cornified lipid envelope
DSC1	desmocollin 1
DSG1	desmoglein 1
ECC	extracellular compartment
FTIR	Fourier transform infrared
IEM	immunoelectron microscopy
NOE	N-oleoylethanolamine
Os-I	osmium tetroxide immersion
Os-V	osmium tetroxide vapor post-fixation
Ru-I	ruthenium tetroxide immersion
Ru-V	ruthenium vapor tetroxide post-fixation
SC	stratum corneum
SSS	swell-shrinkage-slough

REFERENCES

Behne M, Uchida Y, Seki T, et al. Omega-hydroxyceramides are required for corneocyte lipid envelope (CLE) formation and normal epidermal permeability barrier function. J Invest Dermatol. 2000; 114:185–92. [PubMed: 10620136]

Berthaud F, Boncheva M. Correlation between the properties of the lipid matrix and the degrees of integrity and cohesion in healthy human Stratum corneum. Exp Dermatol. 2011; 20:255–62. [PubMed: 21054560]

Brattsand M, Stefansson K, Lundh C, et al. A proteolytic cascade of kallikreins in the stratum corneum. J Invest Dermatol. 2005; 124:198–203. [PubMed: 15654974]

Candi E, Schmidt R, Melino G. The cornified envelope: a model of cell death in the skin. Nat Rev Mol Cell Biol. 2005; 6:328–40. [PubMed: 15803139]

Caubet C, Jonca N, Brattsand M, et al. Degradation of corneodesmosome proteins by two serine proteases of the kallikrein family, SCTE/KLK5/hK5 and SCCE/KLK7/hK7. J Invest Dermatol. 2004; 122:1235–44. [PubMed: 15140227]

Chapman SJ, Walsh A. Desmosomes, corneosomes and desquamation. An ultrastructural study of adult pig epidermis. Arch Dermatol Res. 1990; 282:304–10. [PubMed: 2221982]

Chapman SJ, Walsh A, Jackson SM, et al. Lipids, proteins and corneocyte adhesion. Arch Dermatol Res. 1991; 283:167–73. [PubMed: 1867479]

Christophers E, Kligman AM. Visualization of the cell layers of the stratum corneum. J Invest Dermatol. 1964; 42:407–9. [PubMed: 14172195]

Cork MJ, Robinson DA, Vasilopoulos Y, et al. New perspectives on epidermal barrier dysfunction in atopic dermatitis: gene-environment interactions. J Allergy Clin Immunol. 2006; 118:3–21. quiz 22-3. [PubMed: 16815133]

Downing DT. Lipid and protein structures in the permeability barrier of mammalian epidermis. J Lipid Res. 1992; 33:301–13. [PubMed: 1569381]

Eckert RL, Sturniolo MT, Broome AM, et al. Transglutaminase function in epidermis. J Invest Dermatol. 2005a; 124:481–92. [PubMed: 15737187]

Eckert RL, Sturniolo MT, Broome AM, et al. Transglutaminases in epidermis. Prog Exp Tumor Res. 2005b; 38:115–24. [PubMed: 15746532]

Egelrud T. Desquamation in the stratum corneum. Acta Derm Venereol Suppl (Stockh). 2000; 208:44–5. [PubMed: 10884939]

Elias, P.; Williams, M.; Crumrine, D., et al. Ichthyoses - clinical, biochemical, pathogenic, and diagnostic assessment. Vol. 39. S. Kargar AG; Basel: 2010. p. 144

Elias PM. The skin barrier as an innate immune element. Sem Immunopath. 2007; 29:3–14.

Elias PM, Bonar L, Grayson S, et al. X-ray diffraction analysis of stratum corneum membrane couplets. J Invest Dermatol. 1983; 80:213–4. [PubMed: 6827133]

Elias PM, Choi EH. Interactions among stratum corneum defensive functions. Exp Dermatol. 2005; 14:719–26. [PubMed: 16176279]

Elias PM, Crumrine D, Rassner U, et al. Basis for abnormal desquamation and permeability barrier dysfunction in RXLI. J Invest Dermatol. 2004; 122:314–9. [PubMed: 15009711]

Elias PM, Friend DS. The permeability barrier in mammalian epidermis. J Cell Biol. 1975; 65:180–91. [PubMed: 1127009]

Elias PM, Friend DS, Goerke J. Membrane sterol heterogeneity. Freeze-fracture detection with saponins and filipin. J Histochem Cytochem. 1979; 27:1247–60. [PubMed: 479568]

Elias PM, Goerke J, Friend DS. Mammalian epidermal barrier layer lipids: composition and influence on structure. J Invest Dermatol. 1977; 69:535–46. [PubMed: 925377]

Elias PM, Williams ML, Holleran WM, et al. Pathogenesis of permeability barrier abnormalities in the ichthyoses: inherited disorders of lipid metabolism. J Lipid Res. 2008; 49:697–714. [PubMed: 18245815]

Epstein EH Jr. Williams ML, Elias PM. Steroid sulfatase, X-linked ichthyosis, and stratum corneum cell cohesion. Arch Dermatol. 1981; 117:761–3. [PubMed: 6947719]

Grayson S, Elias PM. Isolation and lipid biochemical characterization of stratum corneum membrane complexes: implications for the cutaneous permeability barrier. J Invest Dermatol. 1982; 78:128–35. [PubMed: 7057048]

Gunathilake R, Schurer NY, Shoo BA, et al. pH-regulated mechanisms account for pigment-type differences in epidermal barrier function. J Invest Dermatol. 2009; 129:1719–29. [PubMed: 19177137]

Hachem JP, Crumrine D, Fluhr J, et al. pH directly regulates epidermal permeability barrier homeostasis, and stratum corneum integrity/cohesion. J Invest Dermatol. 2003; 121:345–53. [PubMed: 12880427]

Hachem JP, Houben E, Crumrine D, et al. Serine protease signaling of epidermal permeability barrier homeostasis. J Invest Dermatol. 2006a; 126:2074–86. [PubMed: 16691196]

Hachem JP, Man MQ, Crumrine D, et al. Sustained serine proteases activity by prolonged increase in pH leads to degradation of lipid processing enzymes and profound alterations of barrier function and stratum corneum integrity. J Invest Dermatol. 2005; 125:510–20. [PubMed: 16117792]

Hachem JP, Roelandt T, Schurer N, et al. Acute acidification of stratum corneum membrane domains using polyhydroxyl acids improves lipid processing and inhibits degradation of corneodesmosomes. J Invest Dermatol. 2010; 130:500–10. [PubMed: 19741713]

Hachem JP, Wagberg F, Schmuth M, et al. Serine protease activity and residual LEKTI expression determine phenotype in Netherton syndrome. J Invest Dermatol. 2006b; 126:1609–21. [PubMed: 16601670]

Haftek M, Serre G, Mils V, et al. Immunocytochemical evidence for a possible role of cross-linked keratinocyte envelopes in stratum corneum cohesion. J Histochem Cytochem. 1991; 39:1531–8. [PubMed: 1717544]

Haftek, M.; Simon, M.; Serre, G.; Elias, PM.; Feingold, KR. Skin Barrier. Taylor & Francis; New York: 2006. Corneodesmosomes: Pivotal Actors in the Stratum Corneum Cohesion and Desquamation; p. 171-190.

Hou SY, Mitra AK, White SH, et al. Membrane structures in normal and essential fatty acid-deficient stratum corneum: characterization by ruthenium tetroxide staining and x-ray diffraction. J Invest Dermatol. 1991; 96:215–23. [PubMed: 1991982]

Houben E, Holleran WM, Yaginuma T, et al. Differentiation-associated expression of ceramidase isoforms in cultured keratinocytes and epidermis. J Lipid Res. 2006; 47:1063–70. [PubMed: 16477081]

Ishida-Yamamoto A, Igawa S, Kishibe M. Order and disorder in corneocyte adhesion. J Dermatol. 2011; 38:645–54. [PubMed: 21545505]

Jonca N, Leclerc EA, Caubet C, et al. Corneodesmosomes and corneodesmosin: from the stratum corneum cohesion to the pathophysiology of genodermatoses. Eur J Dermatol. 2011; 21(Suppl 2): 35–42. [PubMed: 21628128]

Kalinin AE, Kajava AV, Steinert PM. Epithelial barrier function: assembly and structural features of the cornified cell envelope. Bioessays. 2002; 24:789–800. [PubMed: 12210515]

King CS, Barton SP, Nicholls S, et al. The change in properties of the stratum corneum as a function of depth. Br J Dermatol. 1979; 100:165–72. [PubMed: 427018]

Koch PJ, de Viragh PA, Scharer E, et al. Lessons from loricrin-deficient mice. Compensatory mechanisms maintaining skin barrier function in the absence of a major cornified envelope protein. J Cell Biol. 2000; 151:389–400. [PubMed: 11038185]

Long SA, Wertz PW, Strauss JS, et al. Human stratum corneum polar lipids and desquamation. Arch Dermatol Res. 1985; 277:284–7. [PubMed: 4004327]

Lopez O, Walther P, Cocera M, et al. Structural modifications in the stratum corneum by effect of different solubilizing agents: a study based on high-resolution low-temperature scanning electron microscopy. Skin Pharmacol Appl Skin Physiol. 2000; 13:265–72. [PubMed: 10940816]

Lundstrom A, Egelrud T. Evidence that cell shedding from plantar stratum corneum in vitro involves endogenous proteolysis of the desmosomal protein desmoglein I. J Invest Dermatol. 1990; 94:216–20. [PubMed: 1688905]

Lundstrom A, Serre G, Haftek M, et al. Evidence for a role of corneodesmosin, a protein which may serve to modify desmosomes during cornification, in stratum corneum cell cohesion and desquamation. Arch Dermatol Res. 1994; 286:369–75. [PubMed: 7818278]

Mackenzie IC. Ordered structure of the epidermis. J Invest Dermatol. 1975; 65:45–51. [PubMed: 50386]

Madison KC, Swartzendruber DC, Wertz PW, et al. Presence of intact intercellular lipid lamellae in the upper layers of the stratum corneum. J Invest Dermatol. 1987; 88:714–8. [PubMed: 3585055]

Menon GK, Elias PM. Morphologic basis for a pore-pathway in mammalian stratum corneum. Skin Pharmacol. 1997; 10:235–46. [PubMed: 9449162]

Menton DN, Eisen AZ. Structure and organization of mammalian stratum corneum. J Ultrastruct Res. 1971; 35:247–64. [PubMed: 4997548]

Michel S, Schmidt R, Shroot B, et al. Morphological and biochemical characterization of the cornified envelopes from human epidermal keratinocytes of different origin. J Invest Dermatol. 1988; 91:11–5. [PubMed: 2455000]

Naoe Y, Hata T, Tanigawa K, et al. Bidimensional analysis of desmoglein 1 distribution on the outermost corneocytes provides the structural and functional information of the stratum corneum. J Dermatol Sci. 2010; 57:192–8. [PubMed: 20116975]

Nemanic MK, Elias PM. In situ precipitation: a novel cytochemical technique for visualization of permeability pathways in mammalian stratum corneum. J Histochem Cytochem. 1980; 28:573–8. [PubMed: 7190175]

Ohman H, Vahlquist A. The pH gradient over the stratum corneum differs in X-linked recessive and autosomal dominant ichthyosis: a clue to the molecular origin of the “acid skin mantle”? J Invest Dermatol. 1998; 111:674–7. [PubMed: 9764852]

Ovaere P, Lippens S, Vandenabeele P, et al. The emerging roles of serine protease cascades in the epidermis. Trends Biochem Sci. 2009; 34:453–63. [PubMed: 19726197]

Rawlings AV. Recent advances in skin ‘barrier’ research. J Pharm Pharmacol. 2010; 62:671–7. [PubMed: 20636853]

Rawlings AV, Scott IR, Harding CR, et al. Stratum corneum moisturization at the molecular level. J Invest Dermatol. 1994; 103:731–41. [PubMed: 7963664]

Rehfeld SJ, Plachy WZ, Williams ML, et al. Calorimetric and electron spin resonance examination of lipid phase transitions in human stratum corneum: molecular basis for normal cohesion and abnormal desquamation in recessive X-linked ichthyosis. J Invest Dermatol. 1988; 91:499–505. [PubMed: 2844913]

Robinson NA, Lapic S, Welter JF, et al. S100A11, S100A10, annexin I, desmosomal proteins, small proline-rich proteins, plasminogen activator inhibitor-2, and involucrin are components of the cornified envelope of cultured human epidermal keratinocytes. J Biol Chem. 1997; 272:12035–46. [PubMed: 9115270]

Schmuth M, Fluhr JW, Crumrine DC, et al. Structural and functional consequences of loricrin mutations in human loricrin keratoderma (Vohwinkel syndrome with ichthyosis). J Invest Dermatol. 2004; 122:909–22. [PubMed: 15102081]

Scott IR, Harding CR. Filaggrin breakdown to water binding compounds during development of the rat stratum corneum is controlled by the water activity of the environment. Dev Biol. 1986; 115:84–92. [PubMed: 3516761]

Segre J. Complex redundancy to build a simple epidermal permeability barrier. Curr Opin Cell Biol. 2003; 15:776–82. [PubMed: 14644205]

Shukuwa T, Kligman AM. Disaggregation of corneocytes from surfactant-treated sheets of stratum corneum in hyperkeratosis on psoriasis, ichthyosis vulgaris and atopic dermatitis. J Dermatol. 1997; 24:361–9. [PubMed: 9241964]

Swartzendruber DC, Burnett IH, Wertz PW, et al. Osmium tetroxide and ruthenium tetroxide are complementary reagents for the preparation of epidermal samples for transmission electron microscopy. J Invest Dermatol. 1995; 104:417–20. [PubMed: 7861011]

Uchida Y, Holleran WM. Omega-O-acylceramide, a lipid essential for mammalian survival. J Dermatol Sci. 2008; 51:77–87. [PubMed: 18329855]

Voegeli R, Rawlings AV, Breternitz M, et al. Increased stratum corneum serine protease activity in acute eczematous atopic skin. Br J Dermatol. 2009; 161:70–7. [PubMed: 19416247]

Wertz PW, Downing DT. Ceramidase activity in porcine epidermis. Febs Letters. 1990; 268:110–2. [PubMed: 2384145]

Williams ML. Epidermal lipids and scaling diseases of the skin. Semin Dermatol. 1992; 11:169–75. [PubMed: 1498021]

Williams ML, Elias PM. The extracellular matrix of stratum corneum: role of lipids in normal and pathological function. Crit Rev Ther Drug Carrier Syst. 1987; 3:95–122. [PubMed: 3542246]

Williams ML, Elias PM. From basketweave to barrier. Unifying concepts for the pathogenesis of the disorders of cornification. Arch Dermatol. 1993; 129:626–9. [PubMed: 7683187]

Yagi E, Sakamoto K, Nakagawa K. Depth dependence of stratum corneum lipid ordering: a slow-tumbling simulation for electron paramagnetic resonance. J Invest Dermatol. 2007; 127:895–9. [PubMed: 17110934]

Zeeuwen PL, Cheng T, Schalkwijk J. The biology of cystatin M/E and its cognate target proteases. J Invest Dermatol. 2009; 129:1327–38. [PubMed: 19262604]

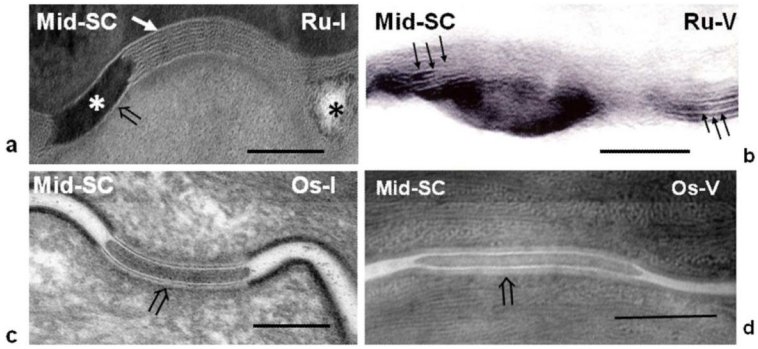

Figure 1. Preservation of Stratum Corneum Structures by Vapor Fixation

Parallel tape strippings and full-thickness skin biopsies were treated with either ruthenium tetroxide or osmium tetroxide vapor fixation (Ru-V and Os-V) (B+D, arrows), or ruthenium tetroxide/osmium tetroxide post-fixation (Ru-I and Os-I, respectively). Arrows indicate lamellar bilayers; open arrows indicate corneodesmosomes (CD), and asterisk indicates extraction artifact. Scale bars = 100 nm.

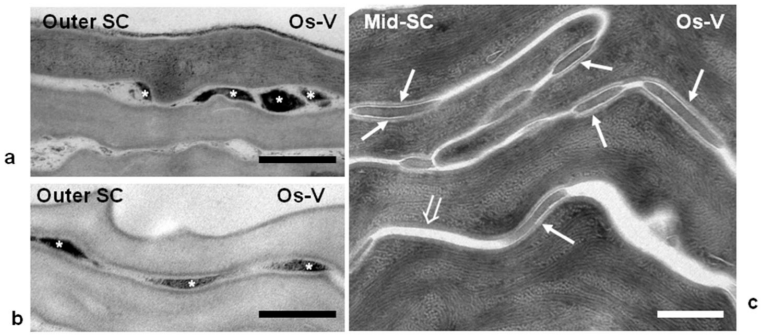

Figure 2. Corneodesmosomes Are Not Present in Outer SC

Tape strippings from outer SC (a+b) and mid-SC (c). Corneodesmosomes (CD) are still present in the mid-SC (c, arrows), but transform into lacunae (a+b, asterisks) in the outer SC. Scale bar, a-c = 200 nm.

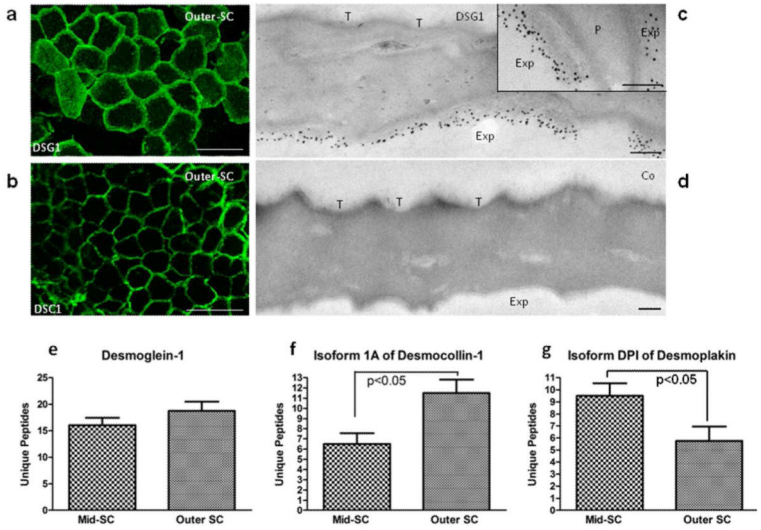

Figure 3. Despite Prior Loss of CD, DSG1 and DSC1 Persist in the Outer SC, and Are Distributed Uniformly in the Cell Periphery

Frozen sections (6 μm) immunostained as in Methods (Suppl Material). a+b: Confocal immunofluorescence images show persistence of desmoglein 1 (DSG1) and desmocollin 1 (DSC1) in the outer SC peripheral membranes. Z-stack of 11 images over 2.5 μm show DSG1 distributed uniformly along basal membranes (not shown). c: Immunoelectron microscopy (IEM) for DSG1 shows uniform distribution of immunogold labeling of cornified envelopes along basal and periphery (c, insert) of corneocytes. Co: Control, Exp: Exposed, P: Periphery, T: Tape. d: Negative control for IEM with omission of primary antibody. e-g: Proteomic analysis of three corneodesmosome proteins (desmoglein 1, desmocollin 1, and desmoplakin) in the mid- and outer SC. Scale bars: a = 50 um, b = 80 um, c (and insert), d = 100 nm.

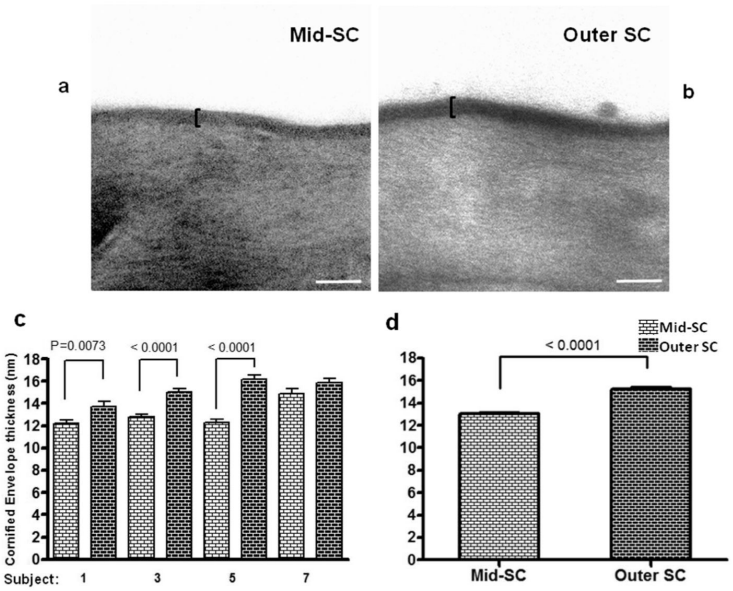

Figure 4. Increased Thickness of Cornified Envelopes during Transit from Mid- to Outer SC

Os-V fixation of mid- and outer SC from four subjects, with quantitation of CE width in perpendicular (cross) sections of randomized, coded micrographs, as described in Methods (Suppl. Material). c: Individual samples, d: pooled data. Scale bar, a+b: = 50 nm.

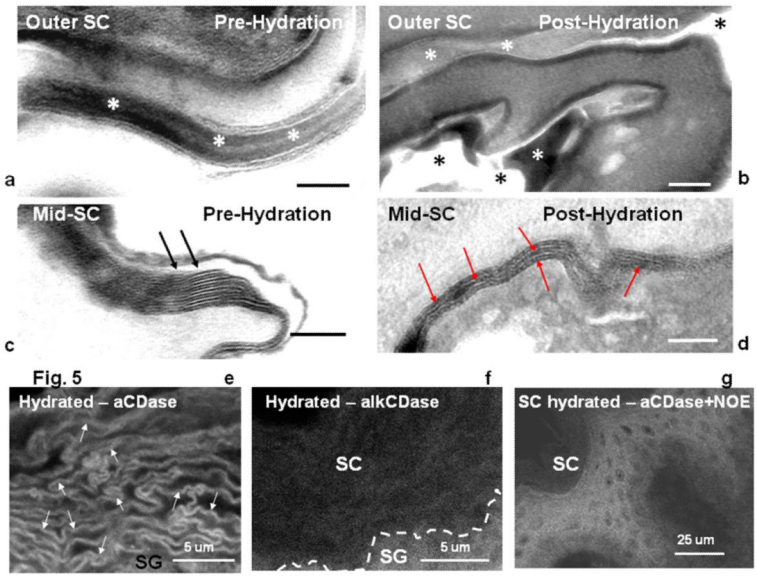

Figure 5. Splitting and Degradation of Lamellar Membranes between Mid- and Outer SC

a+b: Cleft formation (lacunae) and horizontal membrane splitting (a+b, asterisks) Further expansion of clefts, and replacement of water by air, 2 hrs after water immersion (b, asterisks). C+d: Intact lamellar bilayers in mid-SC prior to immersion (c, black arrows), with appearance of punctuate membrane discontinuities that persist at 2 hrs after immersion (d, red arrows). e–g: Confocal microscopy of *in situ* zymography for localization of alkaline and acid ceramidase activity. e: Membrane localization of acidic ceramidase (aCDase) (pH 4.5) in outer stratum corneum (SC, arrows). f: Low levels of alkaline ceramidase (alkCDase) (pH 7.6) activity in SC. g: Reduced enzyme activity in SC after pre-incubations with a pan-ceramidase inhibitor, N-oleoylethanolamine (NOE). a-d, Ru-V fixation. Scale bars: a-d = .25 um; e, f = 5 um; g = 25 um.

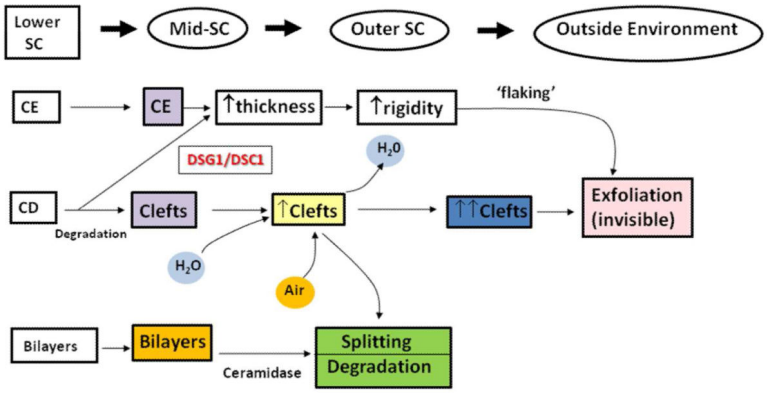

Figure 6.
Basis for Normal Exfoliation: Summary of Observations.